J Mater Sci (2009) 44:4219–4227
DOI 10.1007/s10853-009-3492-x

# Effects of the wrinkled fabric preform on the bending properties of resin transfer molded composites

**Thanh Trung Do · Dong-Joo Lee**

Received: 17 February 2009 / Accepted: 11 April 2009 / Published online: 22 May 2009


**Abstract** During the preform loading of the Resin Transfer Molding (RTM) process, wrinkling in the fabric preform could occur and affect the quality of the bending properties. This study considers the effects that several wrinkled models with different wrinkled lengths in the fabric preforms of K618/R409 and K618/R235 composites have on bending properties. It is found that the experimentally measured values of the bending modulus and strength show a fair agreement with the predicted values using the modified rule of mixtures. Due to the effects of wrinkling, the bending modulus of the wrinkled models is larger than that of the normal model as a function of fiber volume fraction ($V_f$). Based on the energy method, the effects of wrinkling on the bending modulus are determined and described by the wrinkled parameters ($\alpha$). The bending strengths of the wrinkled models have two fracture mechanisms as a function of the ratio of wrinkled length to span length ($L_W/L$). In addition, the safe bending strengths of the wrinkled models are determined.

## Introduction

The Resin Transfer Molding (RTM) process has been widely used in many industries because of its applicability in the production of cost effective, light weight, high specific strength, and specific stiffness composite materials [1–3]. In the RTM process, the fiber preform [3, 4] is first placed into a closed mold, then the polymer matrix is injected in the form of liquid resin through the inlet into the cavity while the remaining air escapes from the mold through the vent [5, 6]. After curing [7], the finished part is demolded. However, wrinkled layers in the fabric preform can easily occur during the preform loading process in the closed mold and can be a source of crack initiation, for which further research is necessary.

Laminar composites also have some inevitable problems due to the wrinkled fabric or discontinued fibers for different geometric shapes, stacking sequences, and material stiffness. Even though the advantages of laminar fabric composites are not proved in terms of their elastic properties, the use of these composites has increased these days due to many advantages such as low manufacturing cost, high fracture toughness, and for their thermodynamic properties and processing techniques. However, due to this wrinkling, the mechanical properties of these composites can also be significantly degraded.

Several researchers have recently worked on the manufacturing and performance of resin transfer molded composites by describing the structure of the fabric preform. Holmberg and Berglund [8] studied the problems of fabric preform of U-beams. They observed that the reinforcement easily lead to a discontinuity in the fabric during preforming and/or mold closure. The discontinuity in the fabric caused the problem of void content within the finished composite. Also, the failure mechanisms of laminar composites due to the stress concentrations were demonstrated by other authors [9–11]. The failure modes could be either the feeling fibers or the breaking fibers depending on the material stiffness, geometrical preform, and area of the interfacial bonding. In addition, the location of the failure

T. T. Do · D.-J. Lee (✉)
School of Mechanical Engineering, Yeungnam University,
214-1, Dae-dong, Gyeongsan-si, Gyeongsan,
Gyeongsangbuk-do 712-749, Korea
e-mail: djlee@yu.ac.kr

T. T. Do
e-mail: thanhtrungspkt@yahoo.com

always occurred at the highest stress concentrations, which influenced the mechanical properties of its composites.

This article examines the effect of wrinkled models with different wrinkled lengths and wrinkled layers on the bending modulus and strength based on the energy method through three-point bend tests. The analytical results are also compared with the experimental data to determine the effects of these wrinkled patterns. In addition, the failure mechanisms as well as the maximum deflection due to the stiffness of materials and failure modes for the wrinkled models are demonstrated.

## Analytical model

A specimen used in the test is modeled as a simply supported beam of a constant thickness, $t$, width, $b$, and span length, $L$. The structure of the specimen has a few wrinkled layers with a wrinkled length of $L_W$. The bending moduli of the wrinkling section are $E_2$ and $G_2$ for the normal and shear factors, respectively. The non-wrinkling sections have bending moduli of $E_1$ and $G_1$ for the normal and shear factors, respectively. For a constant rectangular cross-section, the moment of inertia [12] of the specimen is

$$I = bt^3/12 \tag{1}$$

A three-point bend test is considered, and the specimen is subjected to a load, $P$, applied in its mid-span, as is shown in Fig. 1.

Based on the energy method,

$$\begin{aligned} U_{\text{normal}} &= 2\left(\int_0^{\frac{L}{2}-\frac{L_W}{2}} \frac{M_x^2}{2E_1 I}\mathrm{d}x + \int_{\frac{L}{2}-\frac{L_W}{2}}^{\frac{L}{2}} \frac{M_x^2}{2E_2 I}\mathrm{d}x\right) \\ &= \frac{P^2}{8bt^3}\left(\frac{(L-L_W)^3}{E_1} + \frac{L^3-(L-L_W)^3}{E_2}\right) \end{aligned} \tag{2}$$

$$\begin{aligned} U_{\text{shear}} &= 4\left(\int_0^{\frac{L}{2}-\frac{L_W}{2}}\int_0^{\frac{t}{2}} \frac{\tau^2}{2G_1} b\mathrm{d}y\mathrm{d}x + \int_{\frac{L}{2}-\frac{L_W}{2}}^{\frac{L}{2}}\int_0^{\frac{t}{2}} \frac{\tau^2}{2G_2} b\mathrm{d}y\mathrm{d}x\right) \\ &= \frac{3P^2}{20bt}\left(\frac{L-L_W}{G_1} + \frac{L_W}{G_2}\right) \end{aligned} \tag{3}$$

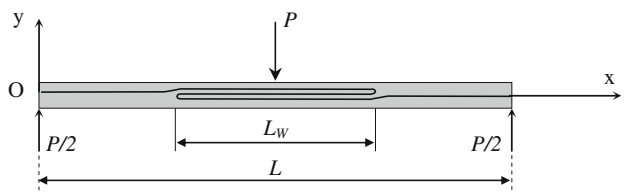


**Fig. 1** Model used in the analytical study

In the three-point bending mode, both the normal and shear stress components are presented throughout the beam span [13]. Therefore, if contributions from both stresses are taken into account, the total energy is

$$\begin{aligned} U &= U_{\text{normal}} + U_{\text{shear}} \\ &= \frac{P^2}{8bt^3}\left(\frac{(L-L_W)^3}{E_1} + \frac{L^3-(L-L_W)^3}{E_2} \right. \\ &\quad \left. + \frac{6}{5}t^2\left(\frac{L-L_W}{G_1} + \frac{L_W}{G_2}\right)\right) \end{aligned} \tag{4}$$

The total deflection at the mid-span of the beam is

$$\begin{aligned} \delta = \frac{2U}{P} &= \frac{P}{4bt^3}\left(\frac{(L-L_W)^3}{E_1} + \frac{L^3-(L-L_W)^3}{E_2} \right. \\ &\quad \left. + \frac{6}{5}t^2\left(\frac{L-L_W}{G_1} + \frac{L_W}{G_2}\right)\right) \end{aligned} \tag{5}$$

The bending modulus as a function of the dimensions, applied load, deflection, and wrinkled length of the specimen is

$$\begin{aligned} &\frac{(L-L_W)^3}{E_1} + \frac{L^3-(L-L_W)^3}{E_2} + \frac{6}{5}t^2\left(\frac{L-L_W}{G_1} + \frac{L_W}{G_2}\right) \\ &= \frac{4\delta bt^3}{P} \end{aligned} \tag{6}$$

where, $G = \frac{E}{2(1+v)}$ and $v$ is a Poisson's ratio. Strictly speaking, this equation can be used for an isotropic material or also used with caution for a material with "fiber" symmetry as in woven or cross-plied at 0° and 90° fiber reinforcement.

The shear pattern can be reduced by employing a high span-thickness ($L/t$) ratio for the beam [13], so Eq. 6 can be rewritten as

$$\frac{(L-L_W)^3}{E_1} + \frac{L^3-(L-L_W)^3}{E_2} = \frac{4\delta bt^3}{P} \tag{7}$$

If the structure of the specimen has no wrinkled layers, i.e., $L_W = 0$ and $E_1 = E_2 = E$, and we ignore the shearing because of the high span-thickness ratio, the above equations can be expressed as given in Eq. 8. Those also can be applied for the general beam without consideration of its structure.

$$\delta = \frac{2U}{P} = \frac{PL^3}{4Ebt^3} \quad \text{and} \quad E = \frac{PL^3}{4\delta bt^3} \tag{8}$$

## Experimental

The materials prepared for this experimental work were Polyester resin R409 (density = 1.12 g/cm$^3$) and R235 (density = 1.05 g/cm$^3$) obtained from the Sewon Chemical Co., and E-glass woven fabric K618 (density = 2.54 g/cm$^3$) obtained from the Hankuk Fibers Co. In order to reduce the

curing time, the hardener material Luperox DDM obtained from Seki Arkema Co., was mixed with the resins, R409 and R235, in the ratio of 1:120 (g).

The specimens used in this study are modeled as a simply supported beam with a rectangular cross-section, which has a thickness of $t = 2.5$ mm and a width of $b = 33$ mm for K618/R409, and a thickness of $t = 2.1$ mm and a width of $b = 33.3$ mm for K618/R235 composite. The geometrical structure of the fabric preform types have several models with different number of layers and wrinkled models with different wrinkled lengths, as is described in the following (Fig. 2):

- Model 1 is a normal type. The fabric preform pattern has different numbers of continuous layers that consists of odd numbers (3, 5, 7, and 9) for K618/R409 and even numbers (2, 4, 6, and 8) for K618/R235 composites.
- Models W-1, W-2, W-3, and W-4 are wrinkled types with different number of layers; 1, 2, 3, and 4, respectively. Typically, the ratios of the wrinkled length to the span length, $L_W/L$, are considered from 0.1 to 0.9.

The size of the original plate sample is 300 mm × 200 mm and test specimens are cut by an electric band saw. Three-point bend tests are performed with a constant span length of $L = 100$ mm, as is shown in Fig. 3. The loads are applied at the mid-span with a speed of 5 mm/min. All tests are done using a Shimazu testing machine at room temperature and a relative humidity of 50%. Typically, three specimens are examined for each sample group from which the mean values are reported.

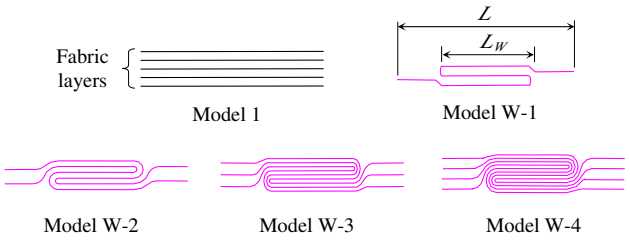


**Fig. 2** Fabric preform models

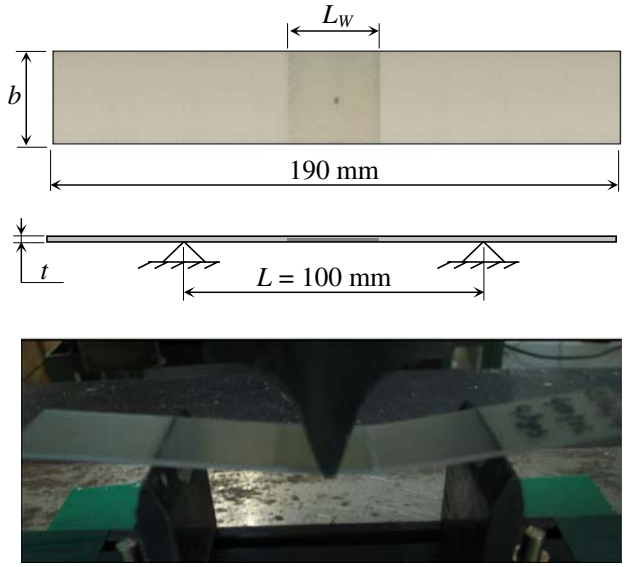


**Fig. 3** Specimen and set-up of a three-point bend test

## Results and discussion

### Bending modulus

In this study, a larger span-thickness ($L/t$) ratio of 40:1 is used and since the effect of energy including shear factor on the general energy was below 3% from the experimental results during the elastic period, the shear factor can be ignored when analyzing the elastic bending modulus. Therefore, the bending modulus can be determined based on the normal stress using Eq. 8. In addition, to consider the effects of the fiber volume fraction in the composite, the bending modulus can be predicted using the modified rule of mixtures [10, 14, 15]:

$$E = C_E E_f V_f + E_m(1 - V_f) \quad (9)$$

where $V_f$ is the fiber volume fraction, $E_m$ and $E_f$ are the moduli of the matrix materials (2.3 GPa for R409 and 3 GPa for R235) and fiber (70 GPa for K618), respectively, and $C_E$ is a fiber efficiency parameter for the bending modulus.

Figure 4 shows the bending modulus of the K618/R409 and K618/R235 composites versus $V_f$. The values of $V_f$ were determined using the density of the matrix, fiber, and composite. Also, in this comparison, half of the measured $V_f$ is used since the effective fibers are only 50% of the fibers in the fabric. The calculated modulus is well matched with the fiber efficiency parameters of 0.62 for K618/R409

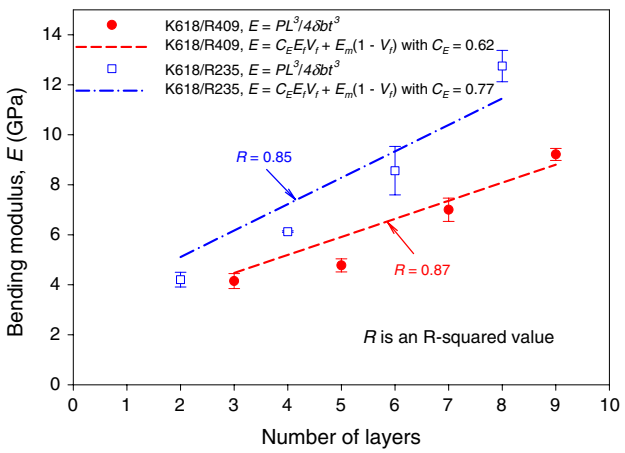


**Fig. 4** Bending modulus of Model 1

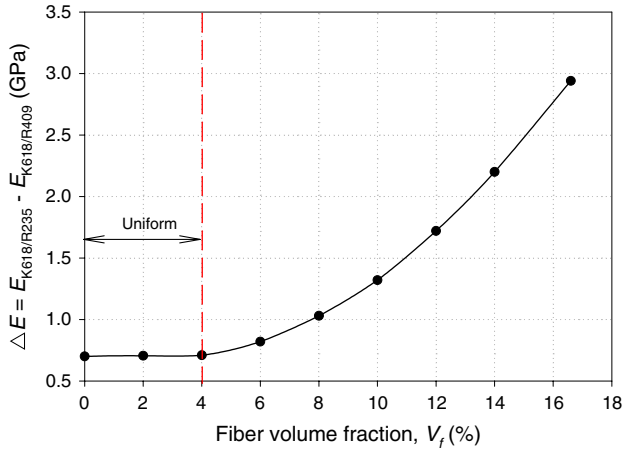


**Fig. 5** Effects of the matrix on bending modulus of Model 1

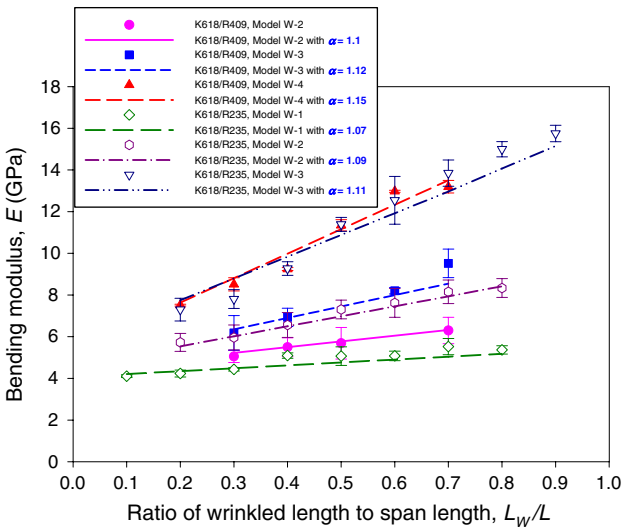


**Fig. 6** Analytical and experimental bending modulus results

and 0.77 for K618/R235. It is believed that this is due to the imperfect interface, matrix viscosity, and fabric type which are not easy to thoroughly wet.

The differences in the bending moduli between the K618/R409 and K618/R235 composites are small, as are shown in Fig. 5. Also, there is no difference in the two matrices ($\Delta = 0.7$ GPa) when $V_f < 4\%$. It is clear that the effects of matrix materials on the bending modulus were very small when $V_f$ was small, but became larger when $V_f$ increased. In addition, the bending modulus always increased as a function of fiber volume fraction [10, 13, 15].

As a function of ratio of the wrinkled length to span length ($L_W/L$), the bending modulus for the whole beam can be calculated using Eq. 8 based on the experimental data for Models W-1, W-2, W-3, and W-4. As expected, the results increased almost linearly with an increasing $L_W$ and have a stiff slope for the wrinkled types with larger number of wrinkled layers in the preform or a higher $V_f$, as is shown in Fig. 6.

In order to consider the effects of the wrinkled length on the bending modulus, Eq. 7 is considered for the relationship between $E_1$ and $E_2$. When $L_W/L = 0$, $E_1 = E$ and $L_W/L = 1$, $E_2 = E$, and in those cases, Eq. 7 can be rewritten as Eq. 8 with those boundary conditions being applied. For $0 < L_W/L < 1$, the experimental bending modulus increased linearly with an increasing wrinkled length. Therefore, the bending modulus can be predicted as the following equation:

$$E = \alpha\left[E_1^*\left(1 - \frac{L_W}{L}\right) + E_2^*\frac{L_W}{L}\right] \tag{10}$$

where $\alpha$ is a wrinkled parameter, $E_1^*$ and $E_2^*$ are the predicted moduli corresponding the non-wrinkling and wrinkling sections, respectively.

We assume that $E_1^*$ and $E_2^*$ are the constant values that can be predicted from the normal preform type (Model 1) with a given number of layers (Fig. 4). For the K618/R409 composite, the predicted values of $E_1^*$are 4 GPa, 4.2 GPa, and 4.6 GPa, and $E_2^*$ are 6.5 GPa, 9.1 GPa, and 14.8 GPa for Models W-2, W-3, and W-4, respectively. Similarly, the predicted values of $E_1^*$ are 3.8 GPa, 4.2 GPa, and 5.1 GPa, and $E_2^*$ are 5.1 GPa, 8.6 GPa, and 14.5 GPa for Models W-1, W-2, and W-3 for the K618/R235 composite, respectively.

Due to the wrinkling pattern and fiber concentration in the wrinkling section where a load $P$ is applied, the fiber volume fraction of the wrinkled models is larger than that of the normal preform as a function of the layers. The modulus of the wrinkling section is also larger than that of the non-wrinkling section, so it can be assumed that $E_1 = \alpha E_1^*$ and $E_2 = \alpha E_2^*$. The wrinkled parameter ($\alpha$) should be a positive number. In those models, the values obtained for $\alpha$ are 1.1, 1.12, and 1.15 for Models W-2, W-3, and W-4 of K618/R409, respectively. For K618/R235, the wrinkled parameters are 1.07, 1.09, and 1.11 for Models W-1, W-2, and W-3, respectively. The trend of the wrinkled parameter tends to increase with an increasing number of wrinkled layers. This happens due to both fiber concentration and geometrical structure of the wrinkled fabric preform. The wrinkled parameter of composite with low-modulus matrix (R409) is larger than that of the composite with high-modulus matrix (R235), which is expected from the same fiber material (K618) and number of wrinkled layers. It is believed that the wrinkled parameter describes not only the effects of wrinkled length and number of wrinkled layers but also the effect of matrix material on the bending modulus. As is shown in Fig. 6, it is clear that the predicted results using Eq. 10 are in good agreement with the analytical results using Eq. 8 and are also satisfied with the experimentally measured data. As expected, the

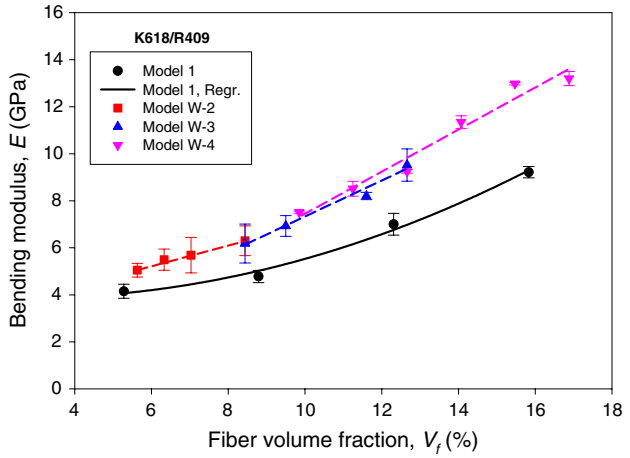


**Fig. 7** Comparison of the bending moduli for K618/R409

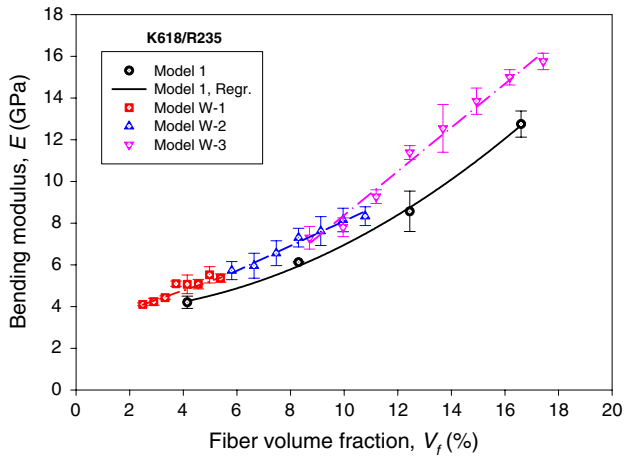


**Fig. 8** Comparison of the bending moduli for K618/R235

bending modulus and wrinkled parameter for the other models with various number of layers and wrinkled lengths can be determined.

Figures 7 and 8 compare the bending moduli of different preform patterns versus fiber volume fraction ($V_f$). Since $V_f$ in the wrinkling section is larger than $V_f$ in the non-wrinkling section of beam, $V_f$ used throughout the beam span of the wrinkled models is averaged from the wrinkling and non-wrinkling sections. It is observed that the bending moduli of the wrinkled models are higher than that of the normal model as a function of $V_f$. This was due to the fiber concentration in the wrinkling section of the composite beam under three-point bend tests. It is clear that the wrinkled preform patterns can be expected in some cases for improving the bending modulus. The bending modulus of the types with a larger number of wrinkled layers in the preform or a higher $V_f$ has a stiff slope for both the K618/R409 and K618/R235 composites (Fig. 9). At the same $V_f$, the bending moduli of the wrinkled models were almost the

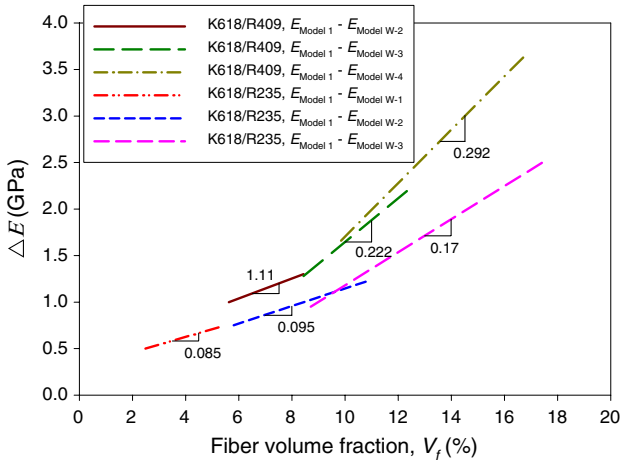


**Fig. 9** Effects of the matrix and wrinkled models on the bending modulus

same even though the number of wrinkled layers varied. In other words, the number of wrinkled layers has only a small effect on the bending modulus. In addition, the K618/R235 with a higher bending modulus of the matrix, 3 GPa, had a smaller differential bending modulus between the normal and wrinkled models than the K618/R409 (bending modulus of the matrix is 2.3 GPa). This is due to the effect of the matrix on the mechanical properties of the RTM composites [16].

## Bending strength

The bending strength with the shear factor in a three-point bend test is given by [13]:

$$\sigma_{\max} = \frac{3P_{\max}L}{2bt^2}\left[1 + 6\left(\frac{\delta}{L}\right)^2 - 4\left(\frac{t}{L}\right)\left(\frac{\delta}{L}\right)\right] \tag{11}$$

To consider the effects of the fiber volume fraction in the composite, the bending strength can be predicted using the modified rule of mixtures [10, 14, 15],

$$\sigma_{\max} = C_\sigma \sigma_f V_f + \sigma_m(1 - V_f) \tag{12}$$

where $\sigma_m$ and $\sigma_f$ are the bending strengths of the matrix materials (45 MPa for R409 and 48 MPa for R235) and fiber (3.4 GPa for K618), respectively, and $C_\sigma$ is a fiber efficiency parameter for the bending strength.

For the different fiber volume fractions for the various number of continuous layers, the bending strength as the maximum stress [4, 11, 16] of the laminate composite specimens for the normal preform as Model 1 was determined and shown in Fig. 10. The experimental results of the bending strength considering the shear factor were higher than that of the simple bending analysis. Also, the predicted values using Eq. 12 were in fair agreement with $C_\sigma$ of 0.28 for K618/R409 and 0.35 for K618/R235. It is also believed

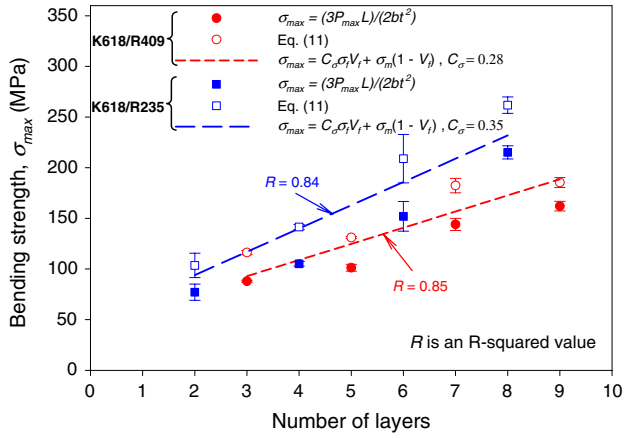


**Fig. 10** Bending strength of Model 1

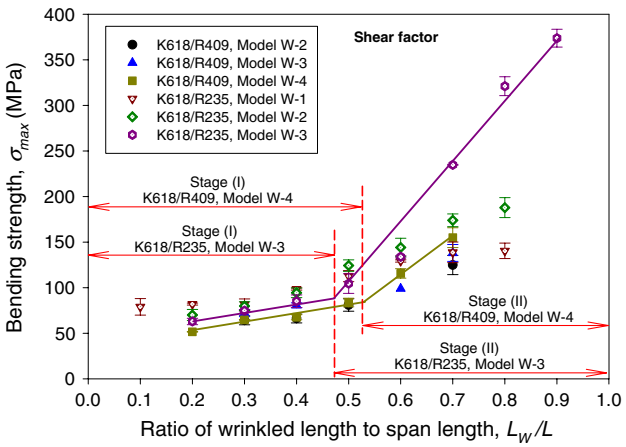


**Fig. 12** Bending strengths of the wrinkled models versus $L_W/L$

that this fair correlation resulted from the poor interface conditions and fabric type reinforcing element.

Figure 11 shows the difference in the bending strengths of K618/R409 and K618/R235 versus $V_f$. Also, the results of the simple bending analysis with and without a shear factor showed a small difference when $V_f < 7\%$. As shown previously, the effects of the matrix on the bending modulus of composites were small in this case, but became wider when $V_f$ increased.

For different wrinkled lengths and models, the bending strengths as the maximum stress of the laminate composite specimens when considering a shear factor were determined, as is shown in Fig. 12. It is shown that the bending strength of the wrinkled models has two stages as a function of $L_W/L$. Stages can be separated as the peeling failure between layers for stage (I) and as the breaking fibers or the achieved maximum fiber stress for stage (II). In those cases, the bending failure loads increased almost linearly with deflection up to the final failure, and the failure pattern had two mechanisms that were due to both the wrinkled length and the model. For the first stage (I), the interface

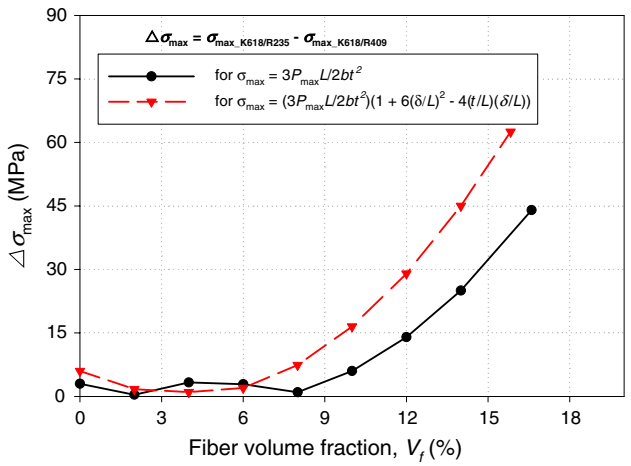


**Fig. 11** Effects of the matrix on the bending strength of Model 1

bond of wrinkled region failed due to $M_W$ (moment of the wrinkling bond area) before the fibers achieved their potential strength, as is shown in Fig. 13a. In this case, Mode I (opening mode) is a main cause of the specimen failure, which occurred at the edge of wrinkling section. The bending strength for fracture may be estimated from the failure load and the failure location in the bending test using simple linear elastic beam analysis as the following equation:

$$\sigma_{\max} = \frac{M_W}{I} r = \frac{3P_{\max} L_W}{bt^2}\left(1 - \frac{L_W}{2L}\right) \tag{13}$$

where $r$ is the half-depth of beam, $r = 0.5t$, $M_W$ is the bending moment of wrinkling bond area, $M_W = [(1 - L_W/2L)P_{\max}](L_W/2)$, and $P_{\max}$ is the maximum load at mid-span length. The highest bending strength occurs at the edge of wrinkling section of the beam.

The peeling failure did not occur when the wrinkled length ($L_W$) reached the critical wrinkled length ($L_{WC}$) that was deemed large enough, i.e., $L_W/L > L_{WC}/L = 0.47$ for Model W-3 of K618/R235 composite and $L_W/L > L_{WC}/L = 0.53$ for Model W-4 of K618/R409 composite (Fig. 12). In those cases, the failures of specimen were due to breaking of fabric or the achieved maximum fiber stress


**Fig. 13** The failure shapes of the wrinkled models

as the second stage (II), which is shown in Fig. 13b. The highest bending moment and failure location occurred at mid-span and its moment was $\frac{P_{\max}L}{4}$. With an assumption that the beam has approximately linear behavior and the shear factor is considered throughout the beam span, the bending strength for fracture at mid-span of beam for this stage can be estimated as the same in Eq. 11. The maximum fiber stress at mid-span of beam may reach the maximum strength.

In general, as a function of the wrinkled length, the bending stress at the edge of wrinkling section is given by the following equation:

$$\sigma_{L_W} = \frac{3P_{\max}L_W}{bt^2}\left(1-\frac{L_W}{2L}\right)\left[1+6\left(\frac{\delta}{L}\right)^2-4\left(\frac{t}{L}\right)\left(\frac{\delta}{L}\right)\right] \tag{14}$$

The bending strength depends on not only the stiffness of materials [4, 10] but also the geometrical structure of the specimen under a three-point bend test. When the wrinkled length is smaller than critical wrinkled length ($L_W < L_{WC}$), the failure strength due to the highest bending moment occurs at the edge of wrinkling section and the bending strength with shear factor can be calculated by Eq. 14. However, when $L_W > L_{WC}$, the bending strength for fracture due to the breaking fibers occurs at mid-span and the stress concentration [9–11] is the largest at its mid-span. Then, the bending strength as the maximum fiber stress in the beam can be calculated by Eq. 11. When $L_W = L$, it means that the structure of the specimen has no wrinkled layers and the boundary condition of Eq. 14 is appropriate to be rewritten as Eq. 11.

From these experimental examinations (Fig. 12), the critical wrinkled length ($L_{WC}$) that needed to transfer from the stage (I) to the stage (II) is obtained with respect to number of wrinkled layers for both composites. Figure 14 shows the critical wrinkled length ($L_{WC}$) versus number of wrinkled layers for two composites, which have different matrix materials. The critical wrinkled length of composite with high-strength matrix (R235) was smaller than that of the composite with low-strength matrix (R409), which is expected from the same fiber material (K618) and number of wrinkled layers. It is believed that the type of fracture depends on not only the number of wrinkled layers or fiber volume fraction but also the stiffness of the specimen under a three-point bend test. In addition, due to the original fabric type with a thickness of 0.18 mm, the maximum number of layers in the wrinkled preform can only be four layers. As expected, this graph can be used to predict $L_{WC}$ for several wrinkled models, which number of wrinkled layers does not exceed four wrinkled layers in the preform, i.e., the predicted results are $L_{WC}/L = 0.34$ for the K618/R409 composite with one wrinkled layer, and

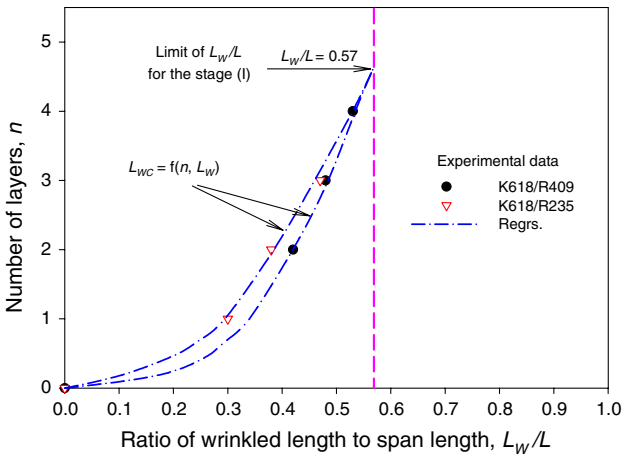


**Fig. 14** Prediction of the critical wrinkled length ($L_{WC}$)

$L_{WC}/L = 0.53$ for the K618/R235 composite with four wrinkled layers in the preform.

As a function of $V_f$, the bending strengths of the normal and wrinkled models were compared for both K618/R409 and K618/R235 by a simple bending analysis with and without a shear factor, as is shown in Figs. 15 and 16. It can be seen that the bending strengths of wrinkled models are almost same as those of the normal models when the wrinkled length ($L_W$) reaches to the safe wrinkled length ($L_{WS}$), which is expected from the same $V_f$. From this, the predicted bending strengths that were safe with wrinkling are determined corresponding to different wrinkled models or number of layers as shown in Fig. 17. For instance, as $L_{WS}/L > L_W/L = 0.42$ for Model W-1 (one layer) of K618/R235 composite, which corresponds to $V_f > 3.4\%$ and $L_{WS}/L > L_W/L = 0.85$ for Model W-4 (four layers) of K618/R409 composite, which corresponds to $V_f > 19\%$, the bending strength with shear factor of its composite was larger than that of the normal model. In addition, the safe

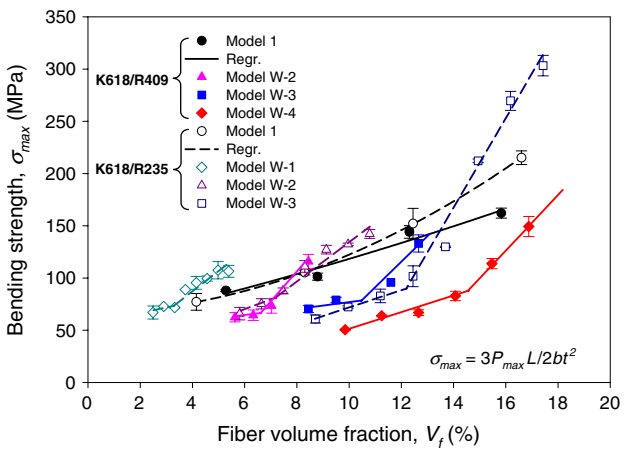


**Fig. 15** Comparison between the wrinkled and normal models for bending strengths without shear factor

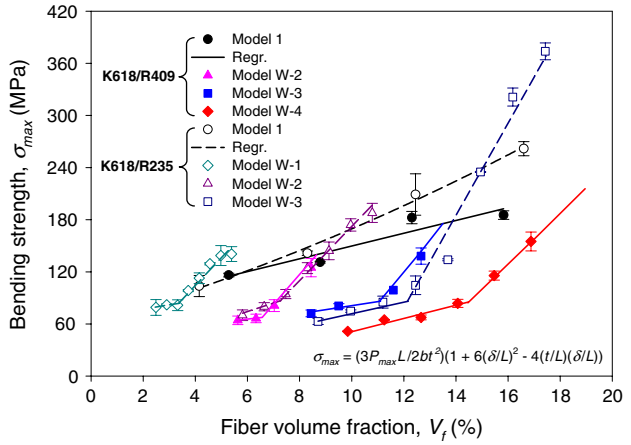


**Fig. 16** Comparison between the wrinkled and normal models for bending strengths when considering shear factor

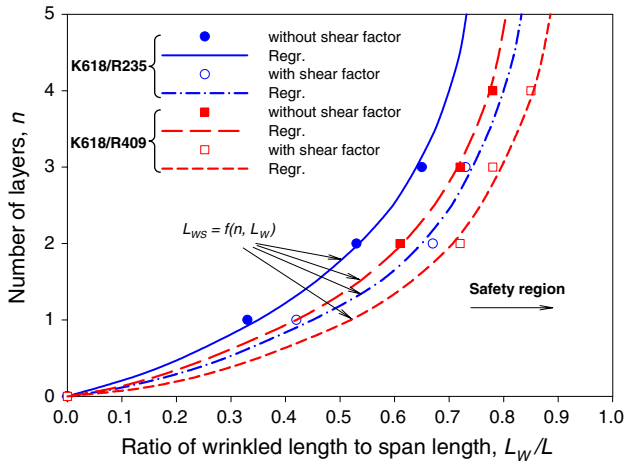


**Fig. 17** The safe wrinkled length ($L_{WS}$) versus the number of layers with different matrix materials

wrinkled length of composite with high-strength matrix (R235) is smaller than that of the composite with low-strength matrix (R409), which is expected from the same fiber material (K618) and fiber volume fraction. It is believed that the safe wrinkled length not only depends on the stiffness of materials but also on the fiber volume fraction of the specimen under a three-point bend test. With a large number of wrinkled layers, the failure strength due to the stiffness and bending moment was large, and sufficient safety of the composite with the wrinkled patterns was expected as the ratio of $L_W/L$ increased.

## Bending deflection

Based on the experimental results, the effects of different preform types on the bending deflection were quite representative for both the cases of normal type with different number of layers and in wrinkled types with different wrinkled lengths. Figure 18 shows the bending deflection of Model 1 (normal preform type) at the maximum load for both K618/R409 and K618/R235. This deflection always decreased with an increasing number of layers. It is clear that the bending deflection of the normal preform decreased with an increasing $V_f$ while satisfying the composite mechanisms. Figure 19 shows the bending deflections of the wrinkled models (Models W-1, W-2, W-3, and W-4) versus the wrinkled length. The results show that the bending deflections at the maximum load, $P_{max}$, have two stages for both K618/R409 and K618/R235. This is due to the failure mode and mechanisms that are caused by both the stiffness and delamination between layers.

Normally, the failure of the laminate composite under a bending test is due to a failure from both compression and tension factors. However, due to the wrinkled fabric that can be assumed as discontinuous fibers in the wrinkled models of W-1, W-2, W-3, and W-4, the failure occurred at

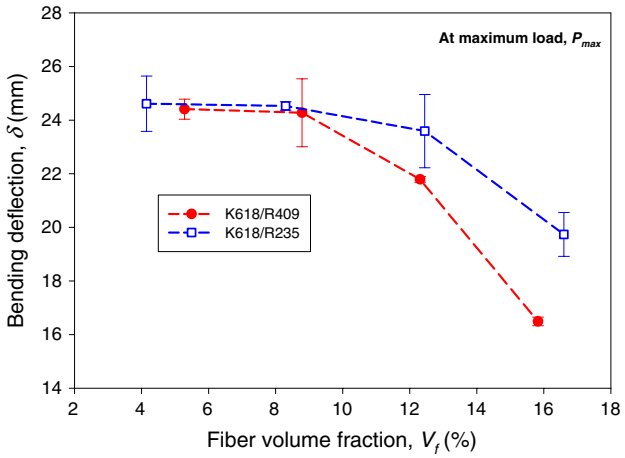


**Fig. 18** Bending deflection of Model 1 at $P_{max}$

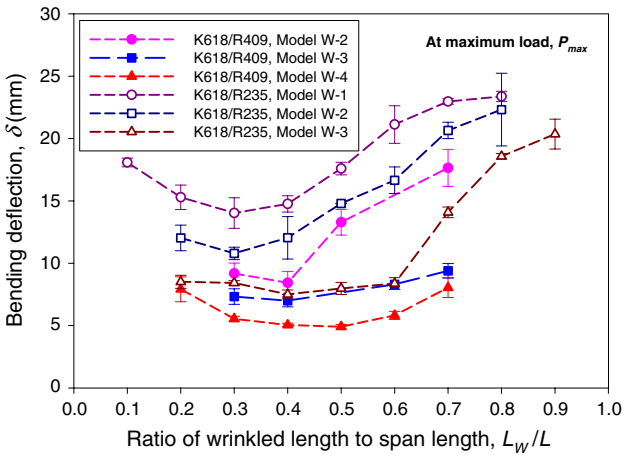


**Fig. 19** Bending deflection of the wrinkled models at $P_{max}$

the edge of the wrinkling section by the primary tension factor at $P_{max}$ for the stage (I). This failure mode was the reason for the small bending deflection in the wrinkled models in comparison with the non-wrinkled model (Model 1). Due to the stiffness of the wrinkling section and the large moment of the wrinkling bond area as $L_W/L$ belongs to stage (I), the specimens were easy to peel at the wrinkling section under the tension factor. This was the reason for the decrease in the deflection with an increasing $L_W/L$. The flexible wrinkling section was larger with an increasing wrinkled length due to the bending mechanisms. In addition, as the wrinkling length increases (period of stage (II)), the moment of the wrinkling bond area and the effects of the failure modes at the edge of wrinkling section were decreased. Therefore, the applied load increased as a function of $V_f$, and the bending deflection increased with an increasing wrinkled length in this period, as is described in Fig. 19.

## Conclusions

The main conclusions drawn from this study were:

- A simple method of analysis is developed to analyze the bending modulus with the wrinkled pattern.
- The experimentally measured values of the bending modulus show a fair agreement with the predicted values using the modified rule of mixtures with the fiber efficiency parameters of 0.62 for K618/R409 and 0.77 for K618/R235 composites. The results of the wrinkled models are larger than that of the normal model. The effects of wrinkling on the bending modulus are described by the wrinkled parameter ($\alpha$), which is due to both the fiber concentration and geometrical fabric preform of the RTM composites.
- The calculated values of the bending strength with the model that considered the shear factor are slightly higher than the calculated bending strength with the simple bending analysis. The experimentally measured values of the bending strength show a fair agreement with the predicted values using the modified rule of mixtures when the fiber effect factor of 0.28 for K618/R409 and 0.35 for K618/R235 composites. The bending strengths of the wrinkled models have two fracture mechanism stages as a function of $L_W$. In addition, the safe bending strengths of the wrinkled models are determined.
- The bending deflection decreases with an increasing number of layers for the normal preform. Due to different failure modes, the bending deflection at the failure load of the wrinkled models show two quite different mechanism stages.

**Acknowledgement** This research was supported by the research grants of Yeungnam University in 2007.

## References

1. Yang B, Kozey V, Adanur S, Kumar S (2000) Compos Part B 31:715
2. Day RJ, Lovell PA, Wazzan AA (2001) Compos Sci Technol 61:41
3. Karlsson KF, Astrom BT (1996) Compos Part A 28:97
4. Swaminathan G, Shivakumar KN, Sharpe M (2006) Compos Sci Technol 66:1399
5. Lawrence JM, Fried P, Advani SG (2005) Compos Part A 36:128
6. Deleglise M, Binetruy C, Krawczak P (2005) Compos Part A 36:339
7. Cheung A, Yu Y, Pochiraju K (2004) Finite Elem Anal Des 40:895
8. Holmberg JA, Berglund LA (1997) Compos Part A 28:513
9. Tong L, Steven GP (1996) Compos Struct 36:91
10. Sreekumar PA, Joseph K, Unnikrishnan G, Thomas S (2007) Compos Sci Technol 67:453
11. Hobbiebrunken T, Hojo M, Adachi T, De Jong C, Fiedler B (2006) Compos Part A 37:2248
12. Dowling NE (1993) Mechanical behavior of materials. Prentice Hall, USA
13. Mallick PK (1998) Fiber-reinforced composites. Marcel Dekker, USA
14. Curtis PT, Blade MG, Bailey JE (1978) J Mater Sci 13:377. doi: 10.1007/BF00647783
15. Jones RM (1975) Mechanics of composite materials. McGraw-Hill, Kogakusha, Japan
16. Zhou Y, Pervin F, Rangari VK, Jeelani S (2006) Mater Sci Eng 426:221